# Supervised Learning of Wireless Signal Waveforms in the Era of Radar-Communications Convergence

Victor Shatov[1], Adela Vagollari[2], Yanpeng Su[1], Wolfgang Gerstacker[2], Maximilian Lübke[1], and Norman Franchi[1]
[1]*Institute for Smart Electronics and Systems*, [2]*Institute of Digital Communications*
*Friedrich-Alexander-Universität Erlangen-Nürnberg, Germany*
Email: {victor.shatov, adela.vagollari, yanpeng.su, wolfgang.gerstacker, maximilian.luebke, norman.franchi}@fau.de

***Abstract*—Widely recognized as a candidate technology for 6G, joint communication and sensing (JCAS) is expected to enable a range of emerging applications in wireless networks. However, incorporating radio sensing capabilities introduces new design challenges and demands novel approaches across various research and engineering disciplines. This paper studies the waveform classification task not only for dedicated communication and radar but also for fully integrated JCAS waveforms. To this end, we generate wireless waveforms that belong to eight classes, including four pure communications standard signal waveforms, two classical radar waveforms, and two fully integrated JCAS candidate waveforms. We examine the dataset's statistical properties and evaluate several machine learning and deep learning classifiers based on expert feature extraction and raw data. Numerical simulations show that expert feature-based classifiers exhibit limited accuracy for the considered task, even for a very high signal-to-noise ratio (SNR). The classifier that learns from raw data yields high accuracy, but requires either a high-performance computing platform or further architectural optimization to meet real-time requirements. Additionally, we investigate the complexity, inference time, and memory footprint of the designed classifiers in the context of their practical implementation in wireless communication systems.**

***Index Terms*—Deep neural network (DNN), joint communication and sensing (JCAS), intelligent spectrum sensing, long short-term memory (LSTM), radar, supervised learning, waveform classification.**

## I. Introduction

THE steadily growing number of wireless Internet of Things (IoT) devices imposes new challenges on the design of the next generation wireless communications standard (6G) [1]. Spectrum sharing and spectrum management tasks are among the most important. In this context, coexistence strategies for communication and radar signals in overlapping frequency bands attracted significant attention [2]. Furthermore, there is significant effort in the research and industry communities on the topic of joint communication and sensing (JCAS), where a stronger integration of communication and radar functionalities is targeted [3]. Specifically, to address the spectrum scarcity issue, there is a paradigm shift in the IoT architecture, where communication and radar tend to merge into a new layer capable of sharing some hardware and wireless resources [4]. As part of JCAS research, new and modified existing waveforms capable of both communication and radar functionalities are under active investigation [5].

Signal recognition is necessary to facilitate the coexistence of various wireless technologies and interference management [6]. This can vary from information regarding the occupancy of a particular channel (e.g., see classical spectrum sensing for cognitive radio) to complete information regarding all transmitters (TXs) and their locations in the area of interest (e.g., for building a digital twin of a radio environment). Sometimes denoted as intelligent spectrum sensing [7], waveform classification, with its variations such as automatic modulation classification (AMC) and radio access technology recognition, plays an essential role in wireless network intelligence [8]. Recently, the importance of signal recognition as one of the promising research directions in JCAS systems was highlighted, among others, in [9]. Specifically, in [9], the authors assumed that the performance and execution time of state-of-the-art JCAS receivers (RXs), which typically process signals using iterative algorithms such as successive interference cancellation, can be improved by machine learning (ML)-based techniques capable of classifying signals by a single look.

Initially performed via feature engineering, the waveform classification task became too complex due to the increased number of wireless standards and modulation types in the air. Therefore, the research community gradually adopted ML techniques ranging from simple decision trees to deep neural networks (DNN) [8]. Many works study the performance of DNN architectures operating on benchmark datasets such as RadioML2018 [10], which comprises multiple communication signals recorded under varying additive white Gaussian noise (AWGN) conditions. To name a few related contributions, [11] focused on computational time reduction, while [12] considered phase imperfections and exploited a convolutional neural network (CNN) for the AMC. In [13], the authors studied an AMC applied to a custom dataset of orthogonal frequency division multiplexing (OFDM)-based communication signals, exploiting an attention-based architecture which combines long short-term memory (LSTM) and convolutional layers. LSTM-based classification for the over-the-air dataset consisting of 6 waveforms is performed in [14].

Recently, spectrum congestion in the sub-6 GHz frequency band has raised interest in waveform classification in the radar-communications coexistence scenario [15]. Furthermore, [16] directly addressed signal classification in the context of JCAS.

However, the studied scenario also falls into the category of coexistence of communication and radar technologies. As of 2025, the wireless community is also exploring the potential of foundation models in the telecommunications industry [17]. Early examples of such models can already be found in relation to positioning [18] and signal recognition [19]. Designed for scalability and minimal calibration effort, the latter, however, only considers well-known communication signals in its dataset.

Radar-communication signal classification remains underexplored. To the best of our knowledge, there are currently no accessible datasets containing samples of signals belonging to emerging wireless systems, such as fully integrated JCAS, nor research addressing the JCAS candidate waveforms for signal classification. Moreover, most of the work on signal classification still considers the AMC task, whereas the more general and complex waveform classification problem remains largely overlooked. Hence, this paper presents a new perspective on wireless signal classification. The main contributions of this work are as follows:

- We generate a novel synthetic dataset comprising IQ samples of multiple realizations of communication, radar, and potential candidate waveforms for fully integrated JCAS under realistic propagation effects for an indoor scenario[1]. The waveforms in the dataset belong to 8 classes. Furthermore, we increase diversity of the dataset considering multiple bandwidths, modulation schemes, coding rates, etc.
- Following the paradigm of explainable ML encouraged by standardization bodies, we then extract a range of popular statistical features for classes in the dataset and investigate their discriminative power. We review knowledge-driven ML techniques for the classification task and adopt them as baseline classifiers.
- We design a DNN that takes raw IQ data as input. Through numerical simulations, we compare the accuracy of the implemented classifiers, demonstrating the limitations of feature-based explainable ML methods for a considered challenging task. Specifically, we study the robustness of the waveform classifiers under degrading SNR conditions and compare the performance of our proposed data-driven DNN for different numbers of input IQ samples.
- The real-time implementation potential of the classifiers is evaluated in terms of computational complexity, inference time, and memory footprint. We show that when combined with hardware accelerators, our proposed DNN yields nearly real-time capability, while not requiring much memory.

This paper is structured as follows. In Section II, we introduce the system model and design the dataset used in the following. In Section III, we apply ML approaches for classification that operate on statistical features of waveforms. In Section IV, we design a DNN, which accepts raw data for classification. Section V provides numerical simulation results and a performance comparison of the studied classifiers. Section VI concludes the paper.

[1]To ensure research reproducibility and transparency, the dataset and code are partially available on https://zenodo.org/records/15256999

## II. System Model and Dataset

The equivalent complex baseband signal $s(t)$ observed at the RX can be expressed as

$$s(t) = s_{\text{TX}}(t) * h(t,\tau) + n(t), \tag{1}$$

where $*$ is the convolution operator, $s_{\text{TX}}(t)$ denotes the equivalent complex baseband transmit signal, and $n(t) \sim \mathcal{CN}(0,\sigma_n^2)$ is the corresponding AWGN. Furthermore, since we consider both TX and RX equipped by single antennas, a complex single-input-single-output (SISO) channel impulse response (CIR) $h(t,\tau)$ expressed by $h(t,\tau) = \sum_{i=1}^{N_p}[\alpha_i(t)\delta(t-\tau_i)]$ characterizes the transmission between them, where $N_p$ is the number of resolvable propagation paths, $\alpha_i(t)$ and $\tau_i$ represent the amplitude and delay associated with the $i$-th path, and $\delta(\cdot)$ denotes the Dirac delta function.

To generate a custom dataset, we employ MATLAB Communications Toolbox and Altair WinProp ray tracing software. First, Communications Toolbox is used to generate 4G, 5G, Wi-Fi, and Bluetooth Low Energy standard-compliant waveforms $s_{\text{TX}}(t)$. This tool allows obtaining baseband IQ samples with certain frame structure with distinguished control and data channels, precise piloting schemes, etc. Additionally, we generate linear frequency modulated waveforms (LFMW) with different bandwidths and pulsed waveforms with different duty cycles to exemplify pure radar. JCAS waveforms are currently under active research and have not yet been standardized, leaving a degree of freedom to approach their choice and generation. Two notable waveform candidates for fully integrated JCAS, namely OFDM and phase modulated continuous waveform (PMCW), represent communication- and radar-centric approaches to JCAS, respectively. For OFDM JCAS, we generate a generic baseband representation of the OFDM-modulated signal without any wireless standard compliance. This additionally allows for specifying the subcarrier indices for the pilot signals and to apply random data symbols that might be used for sensing and communication applications, respectively. PMCW is a single-carrier waveform which originates from the radar community. It can be adopted for communication purposes, although limited in achievable data rate and flexibility. We generate PMCW according to our prior work [20]. The generated waveforms and their varying parameters are summarized in Table I.

Second, we employ the Altair Winprop ray tracing tool to generate CIRs $h(t,\tau)$. To this end, we built an indoor scenario with varying TX and fixed RX positions, generating 209 CIRs in total. Note that amplitudes and phases of multipath channels are assumed to be unknown at the RX.

Finally, we resample the generated $s_{\text{TX}}(t)$ and $h(t,\tau)$ at a common sampling rate $F_s = 194.4\,\text{MHz}$ and insert them into (1) to obtain waveform realizations affected by propagation effects. We then normalize the waveforms to unit variance to make the algorithms less sensitive to the scale of features.

The dataset has the structure $\boldsymbol{\mathcal{D}}^{IQ} = \{\mathbf{s}_j^{IQ}, \mathcal{H}_j\}_{j=1}^{L}$, where $\mathbf{s}_j^{IQ} = \begin{bmatrix} s_{j,1}^I & s_{j,2}^I & \dots & s_{j,L}^I \\ s_{j,1}^Q & s_{j,2}^Q & \dots & s_{j,L}^Q \end{bmatrix}$ contains $L$ IQ samples cut starting from a random index of a $j$'s waveform with attached

TABLE I: The dataset waveforms and their parameters.

| Waveform | Variable Parameters |
|---|---|
| 5G NR | Bandwidth: 15, 50, 100 MHz;<br>Sub-carrier spacing: 15, 30 KHz;<br>Modulation scheme: QPSK, 64-QAM, 256-QAM. |
| 4G LTE | Reference channel: R.2, R.8, R.9;<br>Bandwidth: 1.4, 5, 20 MHz;<br>Modulation scheme: QPSK, 16-QAM, 64-QAM. |
| Wi-Fi | Bandwidth: 20, 80, 160 MHz;<br>Modulation scheme: BPSK, QPSK, 64-QAM;<br>Coding rate: 1/3, 6/7. |
| LFMW Radar | Sweep bandwidth: 5 - 6.25 MHz;<br>Sweep direction: both up and down. |
| OFDM JCAS | Modulation scheme: from BPSK to 1024-QAM;<br>Number of subcarriers: 512, 1024, 2048, 4096. |
| PMCW JCAS | Modul. scheme: BPSK, 16-QAM, 32-QAM, 128-QAM;<br>Spreading codes: PRN-sequences, Gold codes. |
| Bluetooth Low Energy | Data rate: 125 Kbps, 500 Kbps, 1 Mbps, 2 Mbps;<br>Modulation index: 0.45—0.55. |
| Pulsed Radar | Pulsewidth: $\{5, 7, 9, 10, 11, 13, 15, 17, 20\}$ ms;<br>Pulse repetition interval: 100 ms. |

label denoting hypothesis $\mathcal{H}_j \in$ {4G LTE, 5G NR, Wi-Fi, LFMW radar, OFDM JCAS, PMCW JCAS, Bluetooth, Pulsed Radar}. The dataset comprises 149040 sequences of baseband IQ samples corresponding to 8 waveform classes and is balanced, that is, the number of waveforms of every class is equal.

## III. Background and Baseline Time-Series Classification Approaches

This section introduces a number of statistical features adopted for various signal classification problems and several feature-based classifiers.

### A. Statistical Waveform Features

We employ time-series statistical features, which represent the underlying structure of the signal. To this end, we first calculate a set of higher order moments (HOMs), defined for a complex-valued input sequence $s$ as

$$M_{pq} = \mathbb{E}[s^{(p-q)} \cdot (s^*)^q]. \tag{2}$$

Second, we calculate a set of higher order cumulants (HOCs) denoted as $C$ using combinations of HOMs[2]. In total, we extract 14 features to characterize input signals: $M_{20}$, $M_{21}$, $M_{40}$, $M_{41}$, $M_{42}$, $M_{60}$, $M_{80}$, $C_{20}$, $C_{21}$, $C_{40}$, $C_{41}$, $C_{42}$, $C_{63}$, and $C_{80}$. Sets of these features can be seen as a reduced-dimensional representation of a raw signal of any length.

Fig.1 shows normalized histograms that approximate pdfs of the underlying distribution of real-valued cumulants $C_{21} = \mathbb{E}[|s|^2]$ and $C_{42} = M_{42} - |M_{20}|^2 - 2M_{21}^2$. Note that none of the presented waveforms is linearly separable based on these features, thus illustrating the complexity of the task at hand.

Fig. 2 shows the scatter plot of the $M_{80}$ feature. $M_{80}$ is, in general, complex-valued, and therefore its classification can be interpreted as separation in a 2D space. Some waveforms, for example, PMCW, have a distinguishable pattern, with many points appearing along the real axis. This is because most realizations

[2]For the complete list of formulas, refer to [21]).

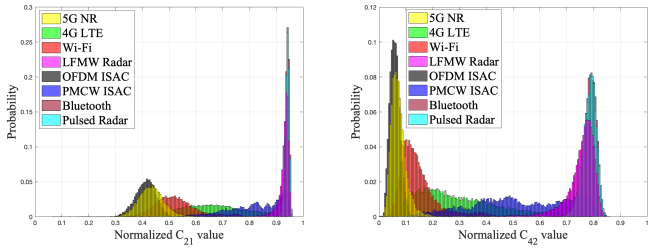


(a) $C_{21}$ (b) $C_{42}$

Fig. 1: Normalized histograms illustrating the probability distribution of statistical features of waveforms in the dataset. One can notice that the presented waveforms are not uniquely linearly separable based on these features.

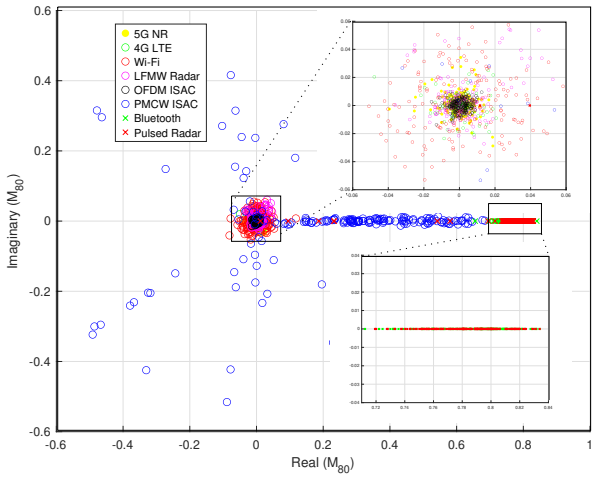


Fig. 2: Scatter plot of normalized statistical feature $M_{80}$ of waveforms in the dataset.

of this radar-centric waveform in the dataset came with BPSK modulation because it ensures good sensing performance. We then note that most of the $M_{80}$ feature values for different waveforms are crammed into a tiny rectangle around the coordinate origin and are hardly separable, clearly exhibiting non-linear class boundaries. Similar patterns hold for the rest of the complex-valued features. Thus, we conclude that it is not possible to obtain an acceptable classification accuracy based on a single feature.

To numerically evaluate feature separability, we use a metric called Bhattacharyya distance (BD). Widely used in statistics and data analysis, BD quantifies the dissimilarity between two probability distributions based on their overlap or shared information. For two discrete probability distributions $P$ and $Q$ in the same domain $\mathcal{X}$, BD is defined as

$$D_B(P, Q) = -\ln\left(BC(P, Q)\right), \tag{3}$$

where $BC(P, Q) = \sum_{x \in \mathcal{X}} \sqrt{P(x)Q(x)}$ is the Bhattacharyya coefficient.

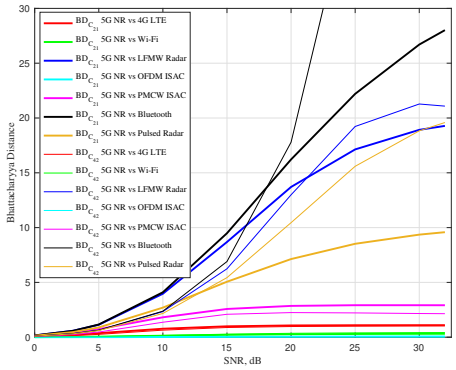


Fig. 3: Pairwise Bhattacharyya Distance between 5G NR and the other 7 considered waveforms based on features $C_{21}$ and $C_{42}$ under varying SNR.

The BD is non-negative, with a value of 0 indicating that the two distributions are identical. A larger BD indicates a greater dissimilarity between the distributions. Fig. 3 shows the BD between 5G NR and the other waveforms in our dataset based on $C_{21}$ and $C_{42}$ for variable SNR, quantitatively supporting the intuition behind Fig. 1.

### B. Baseline Classifiers

To mitigate the non-linearity class boundary problem, we exploit classifiers that operate on input vectors whose entries comprise all the computed features, denoting them as knowledge-driven.

*1) Decision Tree:* Decision tree classification is a popular approach due to its simplicity and interpretability. DTs can separate the decision space into rectangles, shaping relatively complex decision boundaries. The performance of DTs depends mainly on a parameter called maximum depth [22].

*2) Random Forest:* A random forest combines the output of multiple decision trees to obtain a single result by majority vote. Hence, random forests better generalize and reduce overfitting problems but are more computationally expensive. We implement a random forest and a decision tree using the Scikit-learn ML library [22].

*3) Knowledge-Driven DNN:* Inference methods based on domain expert-made features are of great importance due to their explainability and lower complexity [23]. In the context of AMC, small feedforward model-aided DNNs have been used for approximately two decades and are still in use today [24]. Our knowledge-driven DNN accepts 14 features as input. In total, the proposed DNN has six layers of dimensions $14 \times 512$, $512 \times 256$, $256 \times 128$, $128 \times 64$, $64 \times 32$, and $32 \times 8$, respectively, producing the probability metrics associated with 8 waveform classes. After each layer, ReLU is used as an activation function [22]. To train the neural network, we utilize the categorical cross-entropy loss function, realized as

$$\mathcal{L} = -\sum_{n=1}^{N} \log \frac{e^{a_n \cdot \mathcal{H}_n}}{\sum_{k=1}^{K} e^{a_n \cdot k}}, \tag{4}$$

where $N$ is the number of samples in a dataset, $a_n$ are the inputs from the DNN nodes, $\mathcal{H}_n$ are the target labels, and $K = 8$ is the number of classes.

## IV. Data-Driven DNN for Classification

In this section, we design a waveform classifier on IQ samples without any knowledge of the underlying statistical model. Widely used when the data structure is hardly explainable and looks random, such data-driven methods can be seen as a "black box" and categorized as model-agnostic [23]. Model-agnostic methods offer improved flexibility and accuracy at the cost of a high computational burden and lower explainability [25]. Since the waveforms in our case are represented by time series, which inherently exhibit certain temporal patterns, we choose a data-driven architecture based on LSTM layers [26], known for efficiency in the context of related tasks such as AMC [27].

Fig. 4 describes the proposed data-driven DNN architecture. $L$ pairs of IQ samples sequentially enter the DNN and first pass through the two stacked LSTM layers (each has 128 hidden layers). The LSTMs are followed by two fully connected (FC) layers of size $128 \times 256$ and $256 \times 32$, respectively. Finally, the output layer of the classifier has a dimension of $32 \times 8$, where eight neurons correspond to the number of waveforms to learn by the RX. We use categorical cross-entropy defined in (4) as a loss function for training and Adam optimizer with a learning rate of 0.001 [22].

*Remark.* We recognize alternative DNN architectures suitable for the waveform classification task. Specifically, CNN- and Transformer-based architectures have also shown strong performance in various domains. However, CNNs often struggle when applied directly to IQ data. This is because CNNs lack the built-in mechanisms to handle the sequential and long-term structure of time series data, while conversion of data into a spectrogram will require an extra preprocessing step, which consists of multiple overlapping short-time Fourier transforms. This operation is (i) computationally expensive and, therefore, might be impractical, and (ii) loses information on the signal phase [28]. More recent Transformers are widely used to train large language models and are seen as competitors of LSTMs. However, to obtain a justifiable performance gain, they often require larger datasets, longer inputs, and significant computational resources. LSTMs offer a balance between the complexity of the model and the ability to learn long time series dependencies even with limited data, which will be demonstrated in Section V. We leave fine-tuning of our model, as well as implementation of DNNs of other types to further analyze and compare them, for future work.

## V. Numerical Simulation Results

This section provides insight into the accuracy and computational complexity of the classifiers presented in Sections III and IV. The statistical features for the knowledge-based baseline methods were calculated using the input sequence length $L = 256$. The obtained decision tree model has a depth of 13, and the random forest employs 51 estimators, where the hyperparameters were found empirically. For the data-driven classifier, the following

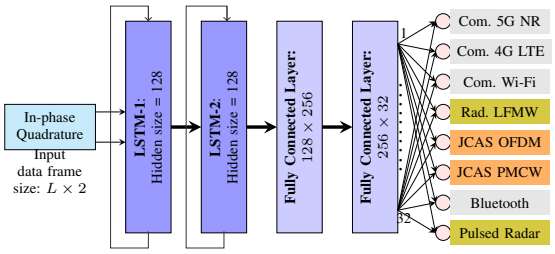


Fig. 4: Illustration of the proposed data-driven DNN architecture. $L$ denotes the length of IQ input sequences.

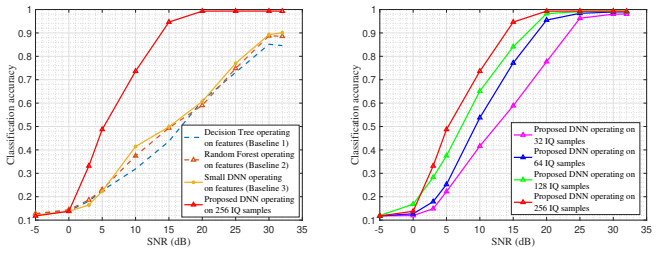


(a) (b)

Fig. 5: Classification accuracy vs. SNR. (a) Decision tree, random forest, knowledge-driven DNN, data-driven DNN with $L = 256$. (b) Data-driven DNN with $L = 32, 64, 128, 256$.

values of the input IQ sequence length were used: 256, 128, 64, and 32. For DNNs, the dataset was divided into 126000 training, 20000 evaluation and 3040 test samples, while to fit the decision tree and random forest models, 90% of the samples were used.

### A. *Performance Comparison*

Fig. 5a compares the classification accuracy of the designed data-driven DNN with raw data input of 256 IQ samples against that of a single decision tree, random forest, and knowledge-driven DNN with input in the form of a vector of statistical features.

We first observe that none of the discussed classification algorithms delivers reasonable performance at very low and negative SNR levels, where the signal's distinguishing characteristics become increasingly obscured by noise. Under such conditions, IQ samples exhibit minimal class-specific structure, converging to Gaussian noise distributions. This is particularly true for OFDM-based signals, which look "random" even when they are noise-free. As a result, the classifier's ability to separate waveform classes deteriorates, approaching random output at SNR below 0 dB[3].

As expected, the accuracy improves with increased SNR for all methods. Data-driven DNN accuracy stands out for all SNR values. For example, at 10 dB, it yields 73.7%, while decision tree, random forest, and knowledge-driven DNN reach only 31.88%, 37.47%, and 41.45% accuracy, respectively. Data-driven DNN yields 90% around 13.5 dB and saturates above 99% after 20 dB. In contrast, three knowledge-driven methods do not cross 85-90% even at the highest SNR values. Fig. 5b shows the classification accuracy of the data-driven DNN for different numbers of IQ samples, namely 256, 128, 64, and 32, used for waveform representation. At very high SNR levels (above 30 dB), there is not much difference in performance for different $L$. However, longer input sequences can improve performance for lower SNR values. For instance, 90% classification accuracy can be achieved for 256, 128, 64, and 32 samples at approximately 13.5 dB, 17 dB, 18 dB, and 23 dB, respectively.

Figs. 6a and 6b show confusion matrices obtained at SNR=20 dB for the data- and knowledge-driven DNNs, respectively. The data-driven model trained and evaluated with 256 IQ samples can perfectly identify 5 waveform classes out of 8. The only relative weakness is the recognition of Wi-Fi, which is in 4.7% of the cases confused with 4G LTE, another OFDM-based communication waveform. The overall classification accuracy is 99.3% for the data-driven DNN and 60.7% for the knowledge-driven DNN. Table II summarizes the other important algorithm evaluation indicators, such as macro-averaged, i.e, computed by averaging the metrics across all classes, precision (Pr.), recall rate (Rec.), and $F_1$ score [22]. As expected, all metrics improve simultaneously with

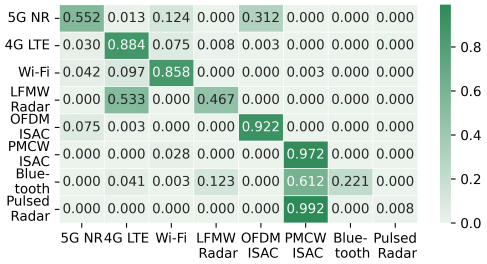


(a) Knowledge-driven DNN.

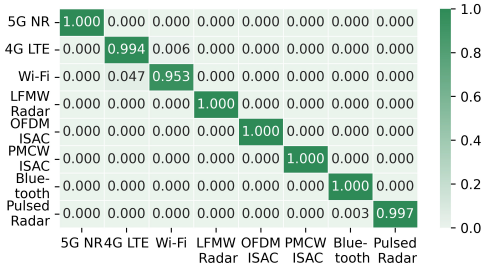


(b) Data-driven DNN.

Fig. 6: Confusion matrices of DNN-based waveform classifiers evaluated at SNR=20 dB.

TABLE II: DNN predictive performance metrics.

| SNR, dB | Knowledge-driven DNN | | | | Data-driven DNN ($L = 256$) | | | |
|---|---|---|---|---|---|---|---|---|
| | Pr. | Rec. | $F_1$ | Acc. | Pr. | Rec. | $F_1$ | Acc. |
| 0 | 0.051 | 0.143 | 0.068 | 0.138 | 0.238 | 0.145 | 0.061 | 0.138 |
| 10 | 0.403 | 0.420 | 0.325 | 0.415 | 0.783 | 0.737 | 0.689 | 0.737 |
| 20 | 0.754 | 0.610 | 0.560 | 0.607 | 0.993 | 0.993 | 0.993 | 0.993 |
| 30 | 0.897 | 0.893 | 0.889 | 0.893 | 0.993 | 0.993 | 0.993 | 0.993 |

[3]The accuracy can be maximized via training a separate model for different SNRs. However, this will significantly increase the overall memory footprint. Alternatively, a single model can be trained using signals with different SNRs. This method can increase the robustness of the model compared to the proposed one, but is generally less stable and predictable and more difficult to train.

increasing SNR.

### B. Complexity and Inference Time

It is crucial to find an adequate balance between algorithm complexity and classification accuracy for a specific application. Table III summarizes the key parameters of the implemented models for a batch of size 128. Inference time was measured on a system with an Intel Core i7-8700 processor and an Nvidia GeForce RTX 2080 graphics card[4]. As expected, decision tree and knowledge-driven DNN operating on waveform features are much faster. However, the real-time capability of the data-driven DNNs which include LSTM layers can be significantly enhanced through GPU-accelerated computations.

The complexity of the considered models is evaluated in terms of learnable parameters as

$$\mathcal{C}_{\text{DNN}} = \sum_{i=1}^{N_{\text{LSTM}}} \underbrace{4(m_i n_i + {n_i}^2 + n_i)}_{\text{LSTM layer compl.}} + \sum_{j=1}^{N_{\text{FC}}} \underbrace{(m_j n_j + n_j)}_{\text{FC layer compl.}}, \quad (5)$$

where $N_{\text{LSTM}}$ denotes the number of LSTM layers, $N_{\text{FC}}$ is the number of FC layers, and $m$ and $n$ are the input and output dimensions of the corresponding $i$-th or $j$-th DNN layer. Although the number of parameters of knowledge- and data-driven DNNs is comparable, it is not the only factor that affects the inference time: the implemented purely data-driven approach relies on LSTM layers whose recursive structure adds complexity. Moreover, the size of the data on which the learned models are applied matters: the inference time for the data-driven architecture is $1.19$ ms and $5.49$ ms for input lengths of $L = 32$ and $L = 256$, respectively. Assuming $1$ ms as a popular threshold to roughly estimate real-time feasibility of the algorithm in modern communication systems [29], we highlight the importance of balancing various design trade-offs and the need to further optimize the DNN parameters for a possible practical implementation.

The storage size required to store the weights, biases, and other relevant parameters of the model is the predominant factor in the total memory footprint. From Table III it can be seen that most models use less than 1 Mb of memory, indicating a small memory footprint and suitability even for resource-constrained embedded systems, with the random forest model being the only exclusion. This is to be expected, as the critical factor that affects memory usage in an random forest is the number of estimators in the forest, which is equal to 51 in our case.

TABLE III: Overview of the complexity, inference time, and requirements on memory size of the designed classifiers.

| Classifier | Number of learn. param. | Memory size (Mb) | CPU inf. time (ms) | GPU inf. time (ms) |
|---|---|---|---|---|
| Decision Tree | N/A | 0.49 | 0.19 | N/A |
| Random Forest | N/A | 153 | 63.52 | N/A |
| Knowl.-driven DNN | 189672 | 0.72 | 0.4 | 0.31 |
| Data-driven DNN ($L = 256$) | 241192 | 0.93 | 76.19 | 5.49 |
| Data-driven DNN ($L = 32$) | 241192 | 0.93 | 7.22 | 1.19 |

## VI. Conclusion

Considering challenges that integration of the radar sensing and communication tasks imposes on wireless systems, this paper studies waveform classification with communication, radar, and fully-integrated JCAS waveforms. We first investigated standard ML-based algorithms that operate on sets of standard expert-crafted features. Through feature discriminability assessment and numerical simulations, we showed that for the task considered, these approaches have limited efficiency. We then implemented a data-driven DNN whose performance was far ahead of baseline knowledge-driven classifiers for all SNR values. Evaluation of the designed data-driven classifier for varying lengths of input data demonstrated the advantage of longer sequences, most notably for low- and medium-SNR conditions. We conclude that despite a trend towards more explainable ML in the wireless community, achieving robust performance on certain tasks requires learning directly from raw data. Future work shall focus on algorithm simplification, e.g., through in-training pruning and quantization techniques, to balance the performance-complexity trade-off to meet real-time requirements and resource constraints of practical applications. Furthermore, amplitude-phase signal representation or spectrograms, combined with diverse architectures, e.g., CNNs or attention-based networks, could be examined. Distributed sensing and federated learning could be leveraged for various purposes, e.g. to improve classification performance in a harsh environment. Finally, datasets captured over the air are required to further evaluate the algorithms.

[4]Detailed hardware-level deployment analysis, including memory access patterns and bandwidth optimization, is beyond the scope of this work.

## Acknowledgment

The authors acknowledge the financial support of the Federal Ministry of Education and Research of Germany (BMBF) via the project “Open6GHub” (grant number: 16KISK005).

## References

[1] X. Chen, D. W. K. Ng, W. Yu, E. G. Larsson, N. Al-Dhahir, and R. Schober, “Massive access for 5G and beyond,” *IEEE J. Sel. Areas Commun.*, vol. 39, no. 3, pp. 615–637, 2021.

[2] L. Zheng, M. Lops, Y. C. Eldar, and X. Wang, “Radar and communication coexistence: An overview: A review of recent methods,” *IEEE Signal Process. Mag.*, vol. 36, no. 5, pp. 85–99, 2019.

[3] V. Shatov et al., “Joint radar and communications: Architectures, use cases, aspects of radio access, signal processing, and hardware,” *IEEE Access*, vol. 12, pp. 47 888–47 914, 2024.

[4] Y. Cui, F. Liu, X. Jing, and J. Mu, “Integrating sensing and communications for ubiquitous IoT: Applications, trends, and challenges,” *IEEE Netw.*, vol. 35, no. 5, pp. 158–167, 2021.

[5] L. Giroto de Oliveira, B. Nuss, M. B. Alabd, A. Diewald, M. Pauli, and T. Zwick, “Joint radar-communication systems: Modulation schemes and system design,” *IEEE Trans. Microw. Theory Tech.*, vol. 70, no. 3, pp. 1521–1551, 2022.

[6] V. Shatov, M. Lübke, Y. Su, and N. Franchi, “On integrated cooperative radio sensing for spatial electromagnetic analysis in 6G,” in *Proc. IEEE Future Networks World Forum (FNWF)*, 2023, pp. 1–8.

[7] N. A. Khalek, D. H. Tashman, and W. Hamouda, “Advances in machine learning-driven cognitive radio for wireless networks: A survey,” *IEEE Commun. Surv. Tutor.*, vol. 26, no. 2, pp. 1201–1237, 2024.

[8] R. Ding, F. Zhou, Q. Wu, C. Dong, Z. Han, and O. A. Dobre, "Data and knowledge dual-driven automatic modulation classification for 6G wireless communications," *IEEE Trans. Wirel. Commun.*, vol. 23, no. 5, pp. 4228–4242, 2024.

[9] F. Liu et al., "Integrated sensing and communications: Toward dual-functional wireless networks for 6G and beyond," *IEEE J. Sel. Areas Commun.*, vol. 40, no. 6, pp. 1728–1767, 2022.

[10] T. J. O'Shea, T. Roy, and T. C. Clancy, "Over-the-air deep learning based radio signal classification," *IEEE J. Sel. Top. Signal Process.*, vol. 12, no. 1, pp. 168–179, 2018.

[11] A. P. Hermawan, R. R. Ginanjar, D.-S. Kim, and J.-M. Lee, "CNN-based automatic modulation classification for beyond 5G communications," *IEEE Commun. Lett.*, vol. 24, no. 5, pp. 1038–1041, 2020.

[12] T. K. Oikonomou et al., "CNN-based automatic modulation classification under phase imperfections," *IEEE Wirel. Commun. Lett.*, vol. 13, no. 5, pp. 1508–1512, 2024.

[13] A. Kumar, M. S. Chaudhari, and S. Majhi, "Automatic modulation classification for OFDM systems using bi-stream and attention-based CNN-LSTM model," *IEEE Commun. Lett.*, pp. 1–5, 2024.

[14] S. Rajendran, W. Meert, D. Giustiniano, V. Lenders, and S. Pollin, "Deep learning models for wireless signal classification with distributed low-cost spectrum sensors," *IEEE Trans. on Cognitive Commun. and Netw.*, vol. 4, no. 3, pp. 433–445, 2018.

[15] G. Kong, M. Jung, and V. Koivunen, "Waveform classification in radar-communications coexistence scenarios," in *Proc. 2020 IEEE Global Commun. Conf. (GLOBECOM)*, 2020, pp. 1–6.

[16] T. Huynh-The, V.-P. Hoang, J.-W. Kim, M.-T. Le, and M. Zeng, "Wavenet: Towards waveform classification in integrated radar-communication systems with improved accuracy and reduced complexity," *IEEE Internet Things J.*, vol. 11, no. 14, pp. 25 111–25 123, 2024.

[17] A. Shahid et al., *Large-scale AI in telecom: Charting the roadmap for innovation, scalability, and enhanced digital experiences*, 2025. arXiv: 2503.04184 [cs.NI]. [Online]. Available: https://arxiv.org/abs/2503.04184.

[18] G. Pan, K. Huang, H. Chen, S. Zhang, C. Häger, and H. Wymeersch, *Large wireless localization model (lwlm): A foundation model for positioning in 6g networks*, 2025. arXiv: 2505.10134 [eess.SP]. [Online]. Available: https://arxiv.org/abs/2505.10134.

[19] M. Cheraghinia, E. D. Poorter, J. Fontaine, M. Debbah, and A. Shahid, *Foundation model for wireless technology recognition using iq timeseries*, 2025. arXiv: 2505.19390 [eess.SP]. [Online]. Available: https://arxiv.org/abs/2505.19390.

[20] Y. Su, V. Shatov, N. Franchi, and M. Lübke, "A code-orthogonal PMCW transmission scheme for improving communications performance in JCAS systems," *IEEE Access*, vol. 12, pp. 29 673–29 689, 2024.

[21] B. Kim, J. Kim, H. Chae, D. Yoon, and J. W. Choi, "Deep neural network-based automatic modulation classification technique," in *Int. Conf. ICT Converg. (ICTC)*, 2016, pp. 579–582.

[22] S. Raschka and L. Yuxi, *Machine Learning with PyTorch and Scikit-Learn: Develop machine learning and deep learning models with Python*. Packt Publishing Ltd., 2022.

[23] N. Shlezinger, J. Whang, Y. C. Eldar, and A. G. Dimakis, "Model-based deep learning," *Proc. IEEE*, vol. 111, no. 5, pp. 465–499, 2023.

[24] Y. Chen, J. He, W. Jiang, Y. Zhang, S. Huang, and Z. Feng, "Toward collaborative and channel-robust automatic modulation classification for OFDM signals," *IEEE Wirel. Commun. Lett.*, vol. 13, no. 11, pp. 3187–3191, 2024.

[25] V. Shatov et al., *Integrated radio sensing capabilities for 6G networks: AI/ML perspective*, 2025. arXiv: 2507.14856 [eess.SP]. [Online]. Available: https://arxiv.org/abs/2507.14856.

[26] S. Hochreiter and J. Schmidhuber, "Long short-term memory," *Neural Computation*, vol. 9, no. 8, pp. 1735–1780, 1997.

[27] S. Ramjee, S. Ju, D. Yang, X. Liu, A. E. Gamal, and Y. C. Eldar, *Fast deep learning for automatic modulation classification*, 2019. arXiv: 1901.05850. [Online]. Available: https://arxiv.org/abs/1901.05850.

[28] W. Zhang, M. Feng, M. Krunz, and A. Hossein Yazdani Abyaneh, "Signal detection and classification in shared spectrum: A deep learning approach," in *Proc. IEEE Conf. on Comput. Commun.*, 2021, pp. 1–10.

[29] R. Wiesmayr, S. Cammerer, F. A. Aoudia, J. Hoydis, J. Zakrzewski, and A. Keller, "Design of a standard-compliant real-time neural receiver for 5G NR," in *Proc. IEEE Int. Conf. on Machine Learning for Commun. and Netw. (ICMLCN)*, 2025, pp. 1–6.